Prediction of Polymer Crystal Structures and Properties. Polyethylene and Poly(oxymethylene)

R. A. Sorensen,† W. B. Liau, L. Kesner, and R. H. Boyd*

Department of Chemical Engineering and Department of Materials Science and Engineering, University of Utah, Salt Lake City, Utah 84112. *Received May 18, 1987*

ABSTRACT: Applying the method described in the preceding paper, molecular mechanics is used to calculate in a unified manner, from transferable conformational energy functions, the packing parameters and energy, vibrational dispersion curves, heat capacity, and thermodynamic functions, elastic constants, and refractive indices of polyethylene (PE) and poly(oxymethylene) (POM). PE was chosen as a "standard" to illustrate the method and POM because it occurs in two crystal forms occasioned by the effect of packing forces in distorting the intramolecular torsion angles and because its crystal properties are of interest. Compared to the free ··GG·· helix, the helix in the orthorhombic form is under compression and that in the hexagonal form under tension. Good agreement between calculated and experimental structures was found. The packing energy of the orthorhombic form is slightly more favorable (1.5 kJ/mol) but the free energies at room temperature are more comparable (0.7 kJ/mol). The calculated heat capacity of POM over the range 100–300 K is in reasonable agreement with the extrapolated experimental values of Gaur and Wunderlich and significantly higher than those of Illers. The C_{33} elastic constant of PE is calculated to be 341 GPa and that of (hexagonal) POM is 83 GPa.

In the preceding paper, a method was described for using molecular mechanics to calculate the packing and properties of polymer molecules. The method allows the crystal packing parameters to be optimized simultaneously with the intramolecular geometry. In the present paper we apply the method to two examples. One of them is polyethylene (PE). It is chosen as a "standard" because its structure and properties are well-known. The other example, poly(oxymethylene) (POM), is chosen to illustrate the utility of the feature of simultaneous *inter-* and *intra*molecular energy minimization. POM crystallizes in two forms. The usually observed form is commonly designated hexagonal. It has been reported[1] as belonging to a trigonal space group with one chain per cell and possessing a helix describable as 9/5 (9 monomers/5 turns) or alternatively as having a threefold screw axis that advances three monomers through $c/3$ via a 120° rotation (Figure 1). The helical advance of one monomer is 200°. The chain internal torsional angles are ~77°. A detailed study[2] indicates that the unit cell possesses hexagonal shape but that the helix may be better described as 29/16. It that case there is no crystal symmetry connected with the helix and the structure would be described as pseudohexagonal. The intramolecular geometry of the 29/16 description is very similar to the 9/5 one.[3] The other crystal form is orthorhombic with two chains per cell.[4] The molecular conformation is a 2/1 helix that advances a monomer by $c/2$ and 180° (Figure 2). The chain internal torsional angles must then be ~63°, assuming the valence angles are slightly larger than tetrahedral.

Although both helices can be described as "all gauche" torsional sequences, the disparity between the torsional angles that allows the two crystal forms to exist is quite striking and illustates the importance of the premise that packing can occasion considerable intramolecular distortion. Thus an important goal of the present work was to determine if energy minimization where the internal degrees of freedom are free to adjust could predict stable structures for both forms. A favorable prognosis comes from a previous calculation by Aich and Haegele[5] in the rigid chain approximation. They concluded that both forms were of comparable stability and that by calculating the energy at a series of fixed torsional angles each form appeared to be stable near its supposed structure. However, it remains to be shown that the structures can be calculated to be stable under general internal deformation. Another important motivation for choosing POM as an example comes from the crystal properties that can be calculated. There has been interest in its heat capacity recently as the result of some disagreement with respect to the values for the crystalline phase that are obtained from extrapolation of experimental values versus crystallinity.[6-9] Thus an apriori calculation based on a force field that successfully calculates vibrational spectra and packing should be valuable in resolving discrepancies. There is also interest in modeling semicrystalline polymers as composites[10-13] and the elastic constants of POM are welcome in this context as input to the models.

Conformational Energy Parameters

Valence Force Field. The molecular mechanics force fields used in this work were intended to produce reasonably good quality vibrational frequencies in addition to the inter- and intramolecular geometries and energies connected with the packing. The inclusion of interaction terms between valence coordinates, such as stretch–bend, stretch–stretch, and bend–bend, is essential in accomplishing this. Without such terms some vibrational frequencies can be as much as 200 cm^{-1} in error. A force-field form similar to that of Snyder and Shachtschneider[14,15] was adopted and parameterized against a data base of assigned frequencies. It differs somewhat in form from the one used by Snyder and Shachtschneider in that nonbonded functions were superposed over the valence forces. The nonbonded function parameters did not participate in the vibrational parameter optimization but the presence of the overlaid nonbonded functions of course did affect the parameterization of the valence field. An iterative least squares procedure was used where a set of frequency displacements as a function of parameter changes was used to minimize the residual of the calculated and experimental frequencies of the data base. The frequency displacements were calculated by the usual perturbation method. The unperturbed mass weighted eigenvectors, $\mathbf{V}_0$, of the dynamical matrix $\mathbf{C}$, give the eigenvalues, λ_0,

$$\mathbf{V}_0{}^t\mathbf{C}\mathbf{V}_0 = \lambda_0$$

and the shifts of λ_0 with the parameter p_k are approximated by

$$\mathbf{V}_0{}^t\partial\mathbf{C}/\partial p_k\mathbf{V}_0 \cong \partial\lambda_0/\partial p_k$$

† Present address: Systems Technology Division, IBM Corp., Austin, TX 78758.

0024-9297/88/2221-0200$01.50/0

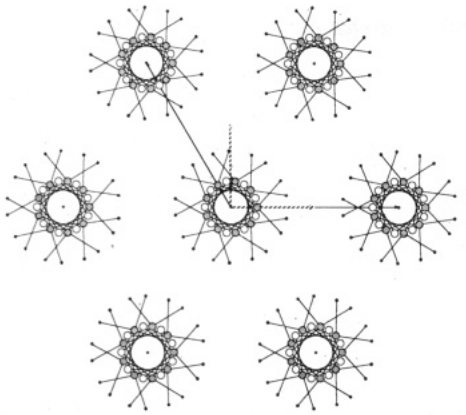

Figure 1. Hexagonally packed poly(oxymethylene), 9/5 helix.

Table I
Valence Potentials for Bond Stretching and Bending[a]

type	k	R^0 or Θ^0	$R_1{}^0$	$R_2{}^0$	$k_{R1,\theta}$	$k_{R2,\theta}$	$k_{R1,R2}$
C–C	4.29	1.53					
C–H[b]	4.70	1.09					
C–H[c]	4.55	1.09					
C–C–H	0.596	1.9106	1.53	1.09	0.2234	0.0	0.0
H–C–H	0.535	1.8832	0.0	0.0	0.0	0.0	0.0
C–C–C	0.747	1.9373	1.53	1.53	0.3537	0.3537	0.1803
O–C	5.133	1.41					
O–C–C	0.827	1.9106	1.41	1.53	0.306	0.599	0.308
C–O–C	1.032	1.9106	1.41	1.41	0.381	0.381	0.135
O–C–H	0.776	1.9106	1.41	1.09	0.277	0.0	0.0
O–C–O[d]							

[a] For stretching, $V = {}^1/_2k(R - R^0)^2$; for bending $V = {}^1/_2k(\theta - \Theta^0)^2 + k_{R1,\theta}(R_1 - R_1{}^0)(\theta - \Theta^0) + k_{R2,\theta}(R_2 - R_2{}^0)(\theta - \Theta^0) + k_{R1,R2}(R_1 - R_1{}^0)(R_2 - R_2{}^0)$, where 1 and 2 refer to first and second bond in type list, R in Å, angles in radians, force constants are in units such that energies are 10^{-18} J/molecule, distances in Å, and angles in radians. In the alkane parameterization the following molecules were used: ethane; propane; *n*-butane, trans; *n*-butane, gauche; *n*-pentane, all trans; *n*-hexane, all trans; heptane, all trans; isobutane; 2-methylbutane, C_1; 2,3-dimethylbutane, C_2 and C_{2H}; cyclohexane. The assignments were from ref 14 and 15. The standard deviation of the fit was 11 cm^{-1}. In the ether parameterization the following molecules were used: dimethyl ether; methyl ethyl ether trans; diethyl ether, all trans; 1,2-dimethoxyethane, trans gauche trans; 1,4-dioxane; tetrahydropyran; methyl isopropyl ether; diisopropyl ether; 2,5-dimethyl-1,4-dioxane. The assignments were from ref 16. The standard deviation was 19 cm^{-1}. [b] For primary H (CH_3). [c] For secondary and tertiary H. [d] Values for O–C–O are takes as the same as those for O–C–C but $R_2{}^0 = 1.41$.

Two parameterizations were carried out. The first was for an alkane force field. The experimental frequency assignments were those of Snyder and Schachtschneider. The other parameterization was for ethers and followed the work of Zerbi and Snyder[16] and used their assignments. The resulting parameters are listed in Tables I–III. The molecules used in the data base are also listed. Where appropriate in the ethers, force constants of the alkane field were invoked.

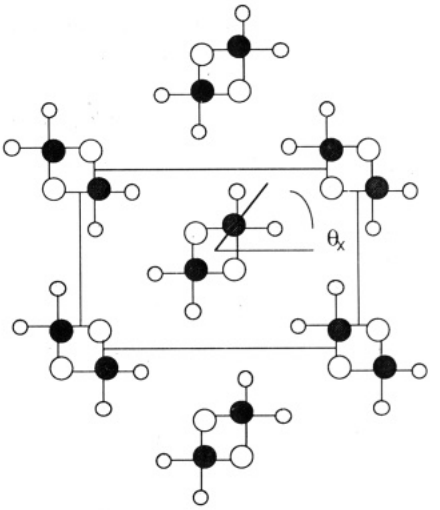

Figure 2. Orthorhombic poly(oxymethylene). Definition of setting angle, θ_x, is also shown.

Nonbonded Functions. The hydrocarbon functions used by us in a number of previous investigations were used again here. It is an "exp-6" formulation based on those determined by Williams[17] and slightly modified by us. The O···O function paramerization is obviously important in the present work on POM. As we have not previously adopted parameters for it we determined them from the experimental data on POM itself. This was done independently from all other parameterizations carried out. It was accomplished by means of preliminary, rigid chain calculations on the hexagonal and orthorhombic forms where experimental lattice parameters and lattice energy were fit. A separate comment on obtaining an experimental lattice energy is made below. Combining rules, geometric mean for the premultiplier constants and arithmetic mean for the exponential constant, were used for the O···C and O···H functions. The nonbonded parameters are listed in Table IV.

Electrostatics. The mutual induction model described in the preceeding paper was used to calculate the internal

Table II
Torsional Potentials and Vicinal Bend–Bend Interactions

type	N-fold	V_0	ϕ_{max}	k_G	$\Theta_1{}^0$	$\Theta_2{}^0$	k_T
C–C–C–C	3	0.001 93	0.0	−0.0939	1.9106	1.9106	0.2062
C–C–C–H	3	0.001 93	0.0	−0.0480	1.9106	1.9106	0.1122
H–C–C–H	3	0.001 93	0.0	−0.0460	1.9106	1.9106	0.1068
C–O–C–C[b]	3	0.005 61	0.0	−0.0939	1.9106	1.9106	0.2062
O–C–C–O[b]	3	0.001 93	0.0	−0.0939	1.9106	1.9106	0.2062
O–C–C–H	3	0.001 93	0.0	−0.070	1.9106	1.9106	0.178
C–O–C–H[c]	3	0.005 61	0.0	−0.078	1.9106	1.9106	0.106
O–C–C–C[b]	3	0.001 93	0.0	−0.0939	1.9106	1.9106	0.2062
C–O–C–O[d]	3	0.0	0.0				
C–O–C–O	2	0.007 8	0.0				
C–O–C–O	1	0.007 9	180				

[a] A torsional potential is used about all of the bonds attached to the center two atoms, –C–C– has nine torsions, –C–O– has three. Torsional potential is $V = {}^1/_2V_0[1 + \cos N(\phi - \phi_{max})]$. Vicinal bend–bend interactions occur in a four-bond sequence, A–B–C–D, and have ∠A–B–C interacting with ∠B–C–D and the potential is $V = k(\theta_1 - \Theta_1{}^0)(\theta_2 - \Theta_2{}^0)$; $k = k_G$ if the torsional angle is near G, G', $= k_T$ if near T. Units are such that energies are in 10^{-18} J/molecule, R's in Å, and angles in radians (except for ϕ_{max} which is listed in degrees). To convert V_0 barriers to kcal/mol multiply by 144.0. [b] Vicinal bending interactions were constrained to be the same values during parameter optimization. [c] When used in POM, V_0 for this torsion is lowered slightly to 0.0050. [d] Three torsional terms, V_1, V_2, and V_3, are used at the C–O–C–O bond in POM. See the text for further comment.

Table III
Bend-Bend Interactions about a Tetrahedral Carbon[a]

group	θ_1	θ_2	k
C–CH_3	H–C⌒C	H–C⌒C	−0.033
C–CH_2–C	H–C⌒C	C–C⌒C	−0.0371
	H–C⌒C	H–C⌒C	−0.0225
	H⌒C–C	H⌒C–C	0.018
C–C(CH)–C	C–C⌒C	C–C⌒C	0.1302
	H–C⌒C	C–C⌒C	−0.0371
	H⌒C–C	H⌒C–C	0.018
C–C(C_2)–C	C–C⌒C	C–C⌒C	−0.041
O–CH_3	H–C⌒O	H–C⌒O	−0.0539
C–CH_2–O	H–C⌒C	O–C⌒C	−0.0371
	H–C⌒C	H–C⌒C	0.0397
	H⌒C–O	H⌒C–C	0.0614
	H–C⌒O	C–C⌒O	−0.0371
	H–C⌒O	H–C⌒O	−0.0524
O–C(CH)–C	H–C⌒C	O–C⌒C	−0.0371
	O–C⌒C	C–C⌒C	0.1302
	H⌒C–C	H⌒C–O	0.0614
	H⌒C–C	H⌒C–C	0.0180
	HC⌒C	C–C⌒C	−0.0371
O–CH_2–O	same as C–CH_2–O		
O–C(CH)–O	same as O–C(CH)–C		

[a] There are six valence angles about a tetrahedral carbon atom and 12 possible bend–bend interactions that involve a common bond. The groups listed above give the substituents and next to these are given the angles interacting with the common bond marked by ⌒. The potential is $V = k(\theta_1 - \theta_1^0)(\theta_2 - \theta_2^0)$; θ_1^0, θ_2^0 are taken to be tetrahedral. Except for the methyl group the same bend–bend interactions were parameterized as transferable between the groups. Units are such that energies are in 10^{-18} J/molecule, R's in Å, angles in radians.

Table IV
Nonbonded Parameters[a]

atoms	A	B	C	ϵ	R_{min}	α
C···C	104.0	3.09	4.45	0.396	3.872	11.96
C···H	30.0	3.415	0.96	0.217	3.253	11.18
H···H	18.4	3.74	0.19	0.0410	3.37	12.6
O···O[b]	526.7	4.063	2.77	0.837	3.20	13.0

[a] A, B, and C are constants in $E = Ae^{-BR} - C/R^6$; energy units are 10^{-18} J/molecule; R in Å; ϵ = well depth, kJ/mol; R_{min} = well position, Å; α = steepness parameter. [b] O···C and O···H potentials are constructed from geometric mean for A and C, arithmetic mean for B.

fields, refractive indices, and electrostatic energies. The model uses bond-centered polarizabilities and for each bond type requires bond polarizabilities $\alpha_\parallel$, $\alpha_\perp$, the fractional location along the bond of the center, for example, f(C–H), and the permanent dipole moment, μ^0. The parameterization for alkanes has already been presented.[18] Preserving the appropriate C–C and C–H values in ethers requires determining only the C–O bond values here. Since there is little anisotropy data available for ethers, only mean polarizabilities were used in fitting. Experimental dipole moments were taken from Nelson et al.[19] It was found that the same C–O bond polarizabilities fit all of the ethers well but that a slightly adjusted μ^0(C–O) value for the C–O–C–O environment in trioxane and dimethoxymethane seemed to be called for. As discussed previously[18] and in the preceeding paper, the mutual induction model is used to calculate the electrostatic energy, molecular polarizabilities, and dipole moments after minimization. Atom-centered fixed charges are used in the minimization process to simulate the polar effects on geometry (0.19e and −0.19e on C and O, respectively, for each C–O bond, where e is the electronic charge). The polar parameters are listed in Table V and the fits in Table VI.

Torsional Barrier in the C–O–C–O Bond. It is well-known that the torsional barrier in the C–O–C–O sequence has special characteristics. The principal one is

Table V
Polar Bond Parameters

bond	μ^0, D	$\alpha_\parallel$, Å^3	$\alpha_\perp$, Å^3	f[a]
C–C	0.0	0.303	0.303	0.50
C–H	0.0	0.486	0.486	0.70
O–C	0.98[b]	0.295	0.295	0.50

[a] f is the location of the polarizability center expressed as fractional distance along the bond from the first atom listed to the second. [b] The value 0.90 D is to be used in the C–O–C–O sequence.

Table VI
Data Fit for Polar Bond Parameters for Ethers

compound	α_m(exptl), Å^3[a]	α_m(calcd), Å^3	μ(exptl), D[b]	μ(calcd), D
dimethyl ether	5.19	5.11	1.30	1.30
methyl ethyl ether	6.92	7.06	1.23	1.19
diethyl ether	8.91	9.03	1.15	1.09
1,4-dioxane	8.59	8.45	0	0
trioxane	–	7.29	2.08	2.07
dimethoxymethane	7.75	7.64	see Table VII	

[a] Calculated from tabulated densities and refractive indices. [b] From ref 19.

that the gauche conformation is more stable than the trans. The barrier and the bond conformation geometry have been parameterized numerous times in molecular mechanics calculations (the "anomeric" effect in carbohydrates) and statistical rotational isomeric state calculations on POM. The torsional angle in POM has often been invoked as part of the data against which the parameterization is carried out. However, as pointed out above there are two significantly different values of the torsional angle and it is this very feature that we wish to explain in terms of a torsional energy function and packing forces. Thus we have elected to use only model compound information in the parameterization of the barrier. Three pieces of data have been selected as the crucial ones in accomplishing this. They all concern dimethoxymethane and they are the torsional angle,[20,21] the frequency of the A species torsional frequency observed in the Raman spectrum,[22] and the temperature dependence of the dipole moment.[23] The latter feature was summarized by Uchida et al. as a gauche trans energy difference and this number has been much used. We have parameterized against the dipole moment directly as we have included polar properties in our molecular mechanics methodology. This has the advantage of allowing for the possibility of inductive effects altering the effective bond moments as a function of conformation. The addition of a twofold term to the threefold term in the barrier has been the usual way to introduce the gauche stability over the trans. We have found, however, that the value of V_2 required to produce sufficient gauche trans energy difference (and yet maintain a sufficiently high value of V_3 to fit the torsional frequency) pushes the torsional angle to higher values than observed. Thus we have invoked an additional term, a single-fold V_1. This allows both the observed torsional angle and the dipole moment temperature dependence to be achieved (gauche trans energy difference), along with the torsional frequency. The potential for a C–O–C–O sequence, then, is

$$V(\phi) = \tfrac{1}{2}V_1^0(1 + \cos\phi) + \tfrac{1}{2}V_2^0(1 + \cos 2\phi) + \tfrac{1}{2}V_3^0(1 + \cos 3\phi) \quad (1)$$

In our representation of torsions we use functions about all of the atoms attached to the center bond. Thus there are nine functions about a C–C bond and three about C–O, one C–O–C–O and two H–C–O–C. In parameterizing eq

Table VII
Torsional Barrier Parameterization from Dimethoxymethane

method	ϕ_{min}	ν, cm^{-1}	μ(298 K), D	μ(472 K), D	ΔE, kJ/mol
calcd	66.9°	95	0.68	1.10	8.3
exptl[a]	63°, 66°	96	0.67	1.08	7.3

[a] The torsional angle minimum, ϕ_{min}, is from electron diffraction, ref 20, 21; torsion A species vibration, ν, is from ref 22; dipole moment, μ, and G, T energy difference, ΔE, are from ref 23.

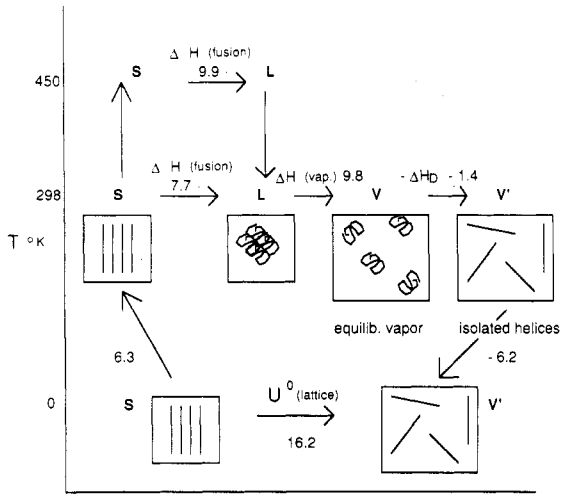

Figure 3. Thermodynamic cycle used to determine the experimental lattice energy of poly(oxymethylene). See text for sources of data.

1 we attempted to leave H–C–O–C the same as in simple ethers. In the fitting process for eq 1 this led to $V_3 = 0$ for C–O–C–O, and in fact a small lowering of V_3 for H–C–O–C in POM was also required. The values of V_1^0, V_2^0, and V_3^0 determined are listed in Table II and the fit to the three key quantities for dimethoxymethane is shown in Table VII.

Lattice Energy of POM. As stated above, the experimental lattice energy of POM was used as an aid in parameterizing the O···O nonbonded function. The derivation of the value from various experimental quantities requires elucidation. The principal pieces of data required and available are the heat of fusion and the heat of vaporization. The former comes from measurements on polymers of known crystallinity.[9] The latter comes from a $-CH_2-O-$ group increment established from heats of vaporization of $CH_3O-(CH_2O)_n-CH_3$ oligomers.[24] The use of these quantities in a thermodynamic cycle to determine the lattice energy is shown in Figure 3. The ancillary data needed are also apparent. The experimental heat of fusion at 450 K of 9.9 kJ/mol (CH_2O)[9] was corrected to 298 K by using the heat capacity of liquid[8] and crystalline[6] POM to arrive at ΔH_{fus} = 7.7 kJ/mol (298 K). The heat of vaporization increment at this temperature is 9.8 kJ/mol.[24] The enthalpy change in bringing the vapor from 0 to 298 K was approximated by the conceptual process of bringing a vapor of isolated GG helices from 0 to 298 K and then disordering the vapor at 198 K to the equilibrium vapor (mixture of conformers).

The enthalpy (=energy) of disordering the vapor at 298 K, ΔH_d, was calculated by using the statistical rotational isomeric state theory.[25] ΔH_d was calculated from the partition function of the vapor, Q, and the free energy, $A = -kT \ln Q$ by using $E = \partial(A/T)/\partial(1/T)$. From rotational isomeric state theory,[25]

$$Q = \tfrac{1}{2}[1 + g(1 + \omega) + [(1 - g(1 + \omega))^2 + 8g]^{1/2}] \quad (2)$$

where $g = e^{-E_G/kT}$, $\omega = e^{-E_\omega/kT}$, and E_G is the gauche energy compared to trans and E_ω is the four-bond GG′ interference energy. The gauche energy was selected to be −6.7 kJ/mol and GG′ sequences were suppressed with $\omega = 0$. With these values, the disordering enthalpy is 1.4 kJ/mol. A vibrational analysis was carried out for the isolated helix and the thermodynamic functions evaluated. The enthalpy at 298 K largely cancels with the value calculated for the crystal, a not unexpected result considering that all but the intramolecular grouplike vibrations have become classical by this temperature. The above data lead to a lattice energy of 16.2 kJ/mol (CH_2O). This value is in fortuitous agreement with one reported in an earlier study[24] that did not have the benefit of an accurate heat of fusion or the means for providing the ancillary data.

Calculations and Results

Calculations were carried out by placing helices on a starting grid and then, as described in the preceding paper, minimizing the energy with respect to the packing parameters along with the internal molecular coordinates. Two starting grids, both of them orthorhombic, were used. One, appropriate for reaching the hexagonal form, contained one chain per cell and the other, appropriate for the orthorhombic POM form and for PE, contained two. In all cases a setting angle was included and in the two chain/cell cases a c axis offset of one chain with respect to the other was included. The nonbonded potential sums were carried out over two complete packing shells (18 chains) about the reference unit. This would apply to both reference units when two chains per unit cell are present.

The choosing of a "repeat" or "reference" unit for the helix requires some comment. It should be chosen large enough so that it includes the complete potential energy environment of the crystal. This would include a unit cell or a smaller unit if a symmetry operation permitted. However, since if predictions of structure are to be made, the c axis size of the cell or the presence of symmetry elements is not known, it is not possible to choose a reference or repeat unit. As an extreme example, in the 29/16 helix for POM, the repeat unit should include all 29 monomers since there is no internal symmetry. In principle, there would be 2 × 29 internal torsional angles that could each have different values. In practice, it is usually, perhaps tacitly, assumed that the polymer helix has a set of internal coordinates, chain torsional and valence angles, for example, that are unique to the monomer chemical repeat unit rather than to the crystal repeat. Thus the 29/16 helix would be assumed to have only one set of C–O–C, O–C–O valence angles and C–O–C–O torsional angles. This amounts to a constraint but such an assumption is the only way calculations could be undertaken without prior knowledge of the structure. We have incorporated this constraint and yet left open the capability for sampling the entire intermolecular potential energy environment of arbitrary helix parameters in the following way. The number of internal valence coordinates chosen and the energy internal to the reference unit are based on one chemical repeat unit. However, in computing the interaction energies of the reference unit with external atoms (nonbonded or electrostatic energy sums), the domain of the reference unit is extended for an arbitrary number of chemical repeat units along the chain. In this way the energy environment can be completely sampled without increasing the number of basis parameters in the energy minimization.

Calculated Structures and Energies. A summary of the geometric packing results is given in Table VIII, the helix parameters are listed in Table IX, and the packing

Table VIII
Calculated and Experimental Lattice Parameters[a]

polymer	a	b	α	β	γ	θ_x	Z_0
PE calcd	7.05	4.94	90.0	90.06	90.0	46.9	0.0
PE exptl[b]	7.15	4.91	90	90	90	~45	0
POM							
hex calcd	7.77	4.50	90.2	90.1	90.3	16°	0
hex exptl[c]	7.74	4.47	90	90	90		0
ortho calcd	7.47	4.81	90.0	89.9	90.2	47.5	0.32
ortho exptl[d]	7.65	4.77	90	90	90		

[a] a, b = unit cell dimensions, Å; α, β, γ = unit cell angles, θ_x = chain setting angle; Z_0 = second chain offset. [b] a and b are low-temperature values from ref 26, θ_x from ref 29, Chapter 7. [c] a and b are values for structure overlaid on orthorhombic grid, $a = 3^{1/2}b$, a(hex) = b; data from ref 1. [d] Data from ref 4.

Table IX
Calculated and Experimental Helix Parameters[a]

polymer	σ	d	θ_1	θ_2	ϕ_1	ϕ_2
PE calcd	180°	1.272	111.9°	111.9°	180°	180°
PE exptl[b]	180°	1.273			180°	180°
POM						
hex calcd	201.4°	1.90	111.4°	109.6°	78.3°	77.9°
hex exptl[c]	198.6°	1.93	112.9°	110.4°	77.0°	77.0°
hex exptl[d]	200°	1.93			78°	78°
ortho calcd	181.8°	1.76	112.7°	111.6°	64.7°	64.5°
ortho exptl[e]	180°	1.78			(~63°)	(~63°)
isolated helix	192°	1.84	112.1°	110.3°	71.7°	71.5°

[a] σ = helix advance angle; d = helix advance distance (Å); θ_1 = C–O–C valence angle; θ_2 = O–C–O valence angle; ϕ_1, ϕ_2 = C–O–C–O torsional angles. [b] Data from ref 29, Chapter 7. [c] 29/16 helix, ref 2 and 3. [d] 9/5 helix, ref 1. [e] Reference 4; torsional angle based on σ = 180° and valence angles calculated here.

Table X
Packing Energetics of POM[a]

contribution	hex	ortho	isolated helix	exptl[b]
intrachain NB	3.7	3.9	3.6	
interchain NB	-14.1	-14.5		
intra ref unit	7.4	6.4	6.5	
ES	26.0	25.7	28.0	
total	23.0	21.5	38.1	
lattice energy, 0 K[c]	15.1	16.6		16.2
free energy, 298 K[d]	-7.2	-6.4		

[a] Units are kJ/mol of $-CH_2O-$; intrachain NB = nonbonded interactions between reference unit and same chain; interchain NB = nonbonded interactions between reference unit and other chains; intra ref unit = intra reference unit energy; ES = electrostatic (dipolar interaction) energy. [b] See text for derivation. [c] The energy under "total" for the isolated helix minus the same quantity for the crystal. [d] Vibrational free energy from Tables XII and XIII.

energies of POM are displayed in Table X. The calculated structure for PE is in good agreement with the experimental one.[26] The isolated chain structure does not differ significantly from that found in the crystal. The calculated packing energy of PE, 16.2 kJ/mol of $-(CH_2CH_2)-$, also agrees well with experiment, 15.4 kJ/mol of $-(CH_2CH_2)-$.[27] For POM, stable structures were found for both the hexagonal form and the orthorhombic one. They also agree well with the experimental ones. The two forms of POM have energies near the experimental value. This of course is conditioned by the fact that preliminary rigid chain calculations were made where the O···O nonbonded function was parameterized with the experimental lattice energy playing a role. A setting angle is reported in Table VIII for hexagonal POM. It was found, however, that although the structure minimized to a value for θ_x the energy is rather insensitive to the actual value.

It is to be observed in Table X that the lattice energy of the orthorhombic form is calculated to be slightly more favorable than that of the hexagonal (by 1.5 kJ/mol).

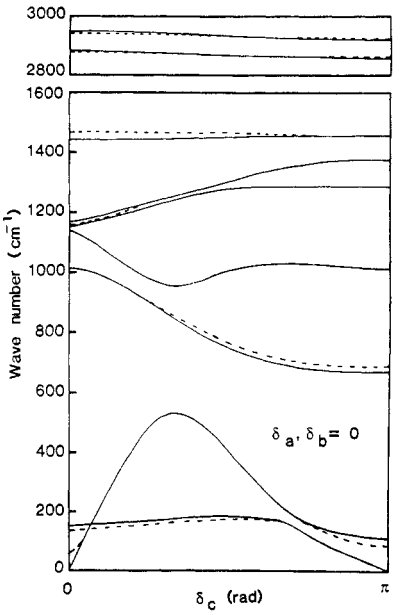

Figure 4. Vibrational dispersion curves for polyethylene plotted along $\delta_c = 0, \pi$ (for $\delta_a, \delta_b = 0$. The dashed curves paired with full ones indicate the splittings due to two chains per cell.

Since both the calculated and observed (from X-ray unit cells) densities are slightly higher for the orthorhombic form, this appears to be a reasonable result. However, it should also be noted that the hexagonal form is calculated to have a slightly more negative vibrational free energy (at room temperature) so that the calculated stabilities differ only very slightly (0.7 kJ/mol). It must be concluded that, within the uncertainties, the stabilities are found to be equal in the present calculation.

It is interesting to notice in Table IX that the isolated helix has a chain torsional angle of ~71°. This is a considerably higher value than that found in dimethoxymethane (Table VII). The infinite helix has significantly more restriction placed on its ability to respond to repulsive close range 1,4- and 1,5-nonbonded interactions than in the two-bond GG sequence in dimethoxymethane. The torsional angles in the isolated free helix are thus midway between those in the two crystal forms. The helix in the hexagonal form is in tension and that in the orthorhombic form is in compression compared to the free helix. This means that neither form is at a marked advantage or disadvantage with respect to the other in a penalty associated with distorting the helix in the crystal. Another point of interest is comparison of the lattice energy of POM with that of PE. Both experimentally and by calculation here they are nearly the same per monomer (although the cohesive energy density is higher for POM due to a smaller molar volume). The nonbonded packing energy is calculated to be slightly lower in POM but this is compensated for by a small dipole–dipole electostatic contribution in POM (~2 kJ/mol, Table X). There is no electostatic contribution in PE as in our parameterization we consider the C–H bond to be nonpolar (Table V).

Vibrational Analysis. The vibrational dispersion curves were calculated as a function of phase angle in all three directions, δ_a, δ_b, and δ_c. It is obviously impractical to display much of this data. For display and discussion purposes the δ_c curve between 0 and π for $\delta_a, \delta_b = 0$ is the most appropriate. These are shown in Figure 4 for PE and Figures 5 and 6 for POM. For PE, the curves seem to be in general agreement with those published by Tasumi and Krimm.[28] The spectroscopically observed optical frequencies which lie at $\delta_c = 0$ and π are in good agreement

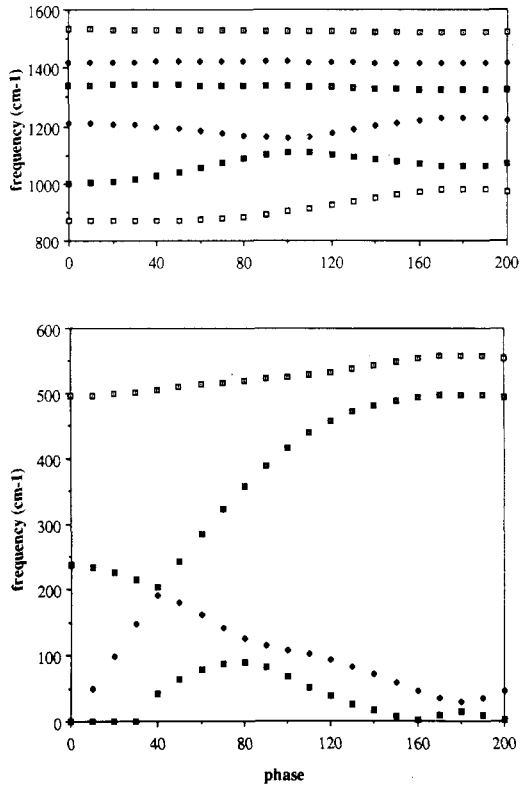

Figure 5. Vibrational dispersion curves for hexagonal poly(oxymethylene) plotted along $\delta_c = 0, 10\pi/9$ for $\delta_a, \delta_b = 0$.

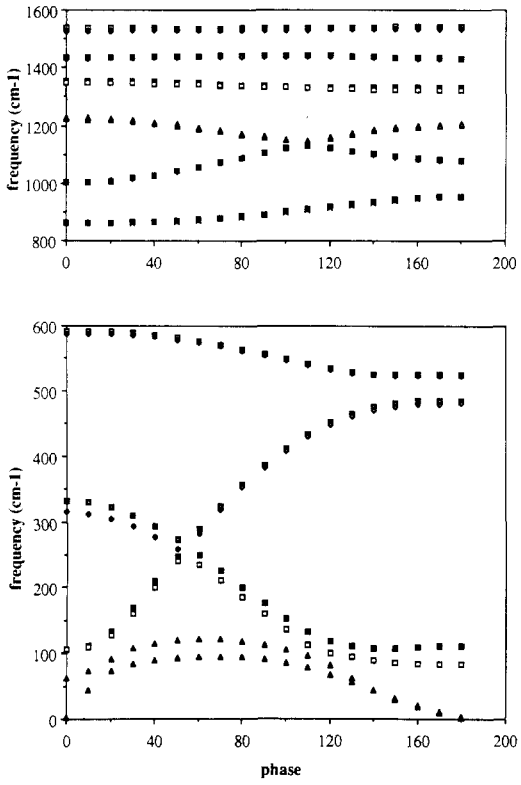

Figure 6. Vibrational dispersion curves for orthorhombic poly(oxymethylene) plotted along $\delta_c = 0, \pi$ for $\delta_a, \delta_b = 0$.

with previous assignments.[29] Lattice modes $\nu(0)$ were calculated to be 46, 140, 158 cm^{-1} and $\nu(\pi)$ to be 80 and 104 cm^{-1}. These are somewhat lower than those calculated by Tasumi and Krimm. That there are differences in these calculated results is not suprising since they depend strongly on the nonbonded potentials and they are quite different between the two works.

Table XI
Elastic Constants[a]

crystal	C_{ij} 1	2	3	C_{44}	C_{55}	C_{66}
PE						
1	14.3	7.2	1.92	3.64	2.27	7.3
2	7.2	12.2	3.30			
3	1.92	3.30	341.			
POM hex						
1	19.2	6.3	16.9	5.8	5.6	6.7
2	6.3	20.2	8.4			
3	16.9	8.4	83.0			
POM ortho						
1	19.5	9.8	9.0	5.0	6.9	10.4
2	9.8	18.7	4.0			
3	9.0	4.0	84.3			

[a] Units are GPa. C_{44} refers to α, α, C_{55} to β, β, etc... S_{33}^{-1} (fiber modulus) calculated from $\mathbf{S} = \mathbf{C}^{-1}$ is 341 PE, 64 POM hex, and 81 POM ortho.

For POM, we were encouraged by the work of Piseri and Zerbi[30] to apply our force field developed for ethers. The modifications made for POM are indicated in Tables I-III. In addition, as stated, special attention was given to parameterizing the torsional barrier for the C–O–C–O sequence (from dimethoxymethane). As could be expected, however, since the force field was primarily parameterized for simple ethers, the nonskeletal optical frequencies (at $\nu(0)$, $\nu(8\pi/9)$, or $\nu(10\pi/9)$ for hexagonal and at $\nu(0)$, $\nu(\pi)$ for orthorhombic) do not agree with the previous assignments[30] as well as they do for PE. Nevertheless the agreement is satisfactory. The general features of the dispersion curves are similar to those found by Piseri and Zerbi for isolated chains. The lattice modes and the two chains per cell splittings for the orthorhomobic form were not of course obtained by them. For the hexagonal form the lattice mode at $\nu(8\pi/9)$ or $\nu(10\pi/9)$ is calculated at 46 cm^{-1}. For the orthorhombic form, lattice modes at $\nu(0)$ were calculated to be 62, 104.9, and 106.3 cm^{-1} and $\nu(\pi)$ to be 80 and 104 cm^{-1}.

Especially pleasing is the fact that the torsonal frequency for hexagonal POM at $\nu(0)$ is calculated to be 236 cm^{-1} versus 235 cm^{-1} observed and that in the orthorhombic form the $\nu(0)$ is calculated at 314, 331 cm^{-1} compared to 304 cm^{-1} observed. The agreement, extending to the dependence on the crystal form, indicates that the skeletal torsional barrier has been well parameterized. In turn this lends confidence to the results of the crystal structure calculations since they depend rather sensitively on the choice of torsional barrier.

Elastic Constants. The elastic constants calculated for PE and hexagonal and orthorhombic POM are listed in Table XI. The values for PE are in agreement with those calculated by Wobser and Blasenbrey[31] and somewhat less so with those of Odajima and Maeda.[32] The fiber modulus is calculated to be 341 GPa. This compares to 325 and 257 GPa reported in ref 31 and 32, respectively. There have been many experimental values from spectroscopic longitudinal acoustic mode measurements. These include 358,[33] 290,[34] and 350[35] GPa.

In POM a longitudinal acoustic mode measurement has been made.[36] The slope of the frequency versus reciprocal lamellar thickness plot is in reasonable agreement with slope of the appropriate dispersion curve calculated here and the one by Piseri and Zerbi.[30] However, when the slope is interpreted in terms of a fiber modulus by using the elastic rod analogy,[36] the modulus is calculated to be much higher than found here, 189 versus 64 Gpa (Table XI). The apparent explanation for this that the elastic rod

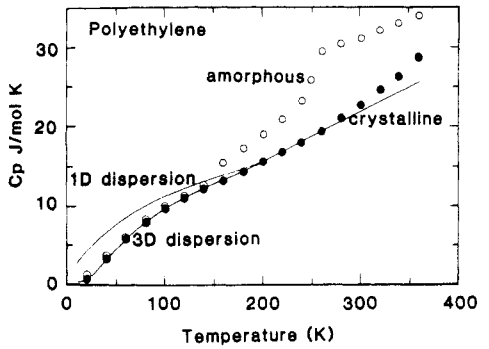

Figure 7. Heat capacity, C_p, versus temperature for polyethylene. Closed circles are taken from experimental data extrapolated to 100% crystallinity and tabulated by Gaur and Wunderlich,[41] open circles are the tabulated extrapolation for amorphous polyethylene. The two curves are calculations based respectively on sampling the vibrational dispersion curves of a single chain (1D) and those for the crystal (3D).

formula is not appropriate for a helix with displacements normal to the chain direction as well as along it. In other words, the normal modes are acoustic in nature but are not purely longitudinal in displacement. An elastic rodlike relation between the dispersion curve slope and chain force constants has been established only for the planar zigzag skeleton.[37] It is difficult to use direct mechanical measurement to establish fiber moduli as the problem of continuity of stress or strain in the invariably semicrystalline samples arises. Measurements of crystal moduli from unit cell distortions in a loaded specimen lead to an lower bound on the crystal fiber modulus when the stress is assumed to be the macroscopic load divided by sample area. Jungnitz et al.[38] have made such measurements on highly oriented POM specimens at low temperature where the moduli of the amorphous and crystalline phases are much closer than at room temperature and the uncertainty from the stress distribution assumption is therefore less. They find a crystal fiber modulus of ~72 Gpa for their highest draw ratio compared to our calculated value of 64 GPa.

Thermodynamic Functions. Thermodynamic functions were evaluated by sampling frequencies from the dispersion curves at evenly spaced intervals along the δ_a, δ_b, δ_c axes. For PE this was 20 × 20 × 20 points and for POM 10 × 10 × 10. The calculated constant volume functions were corrected to constant pressure by using the standard thermodynamic formulation, $C_p - C_v = V\alpha^2T/\beta$. The value $\beta = 0.16$ (GPa)$^{-1}$ found by Sham et al.[39] was used for β for PE. This value compares to $\beta = 0.10$ (GPa)$^{-1}$ calculated from the elastic constants of Table XI (or ref 31) and eq 25 of the preceeding paper. An experimentally derived value[40] of $\alpha = 2 \times 10^{-4}$ K^{-1} was adopted. For POM, the values $\beta = 0.077$ (GPa)$^{-1}$ (hex) and 0.073 (GPa)$^{-1}$ (ortho) were calculated from the elastic constants of Table XI and used. For a lack of a better value of α the same value as for PE was used.

The calculated heat capacity of PE is shown in Figure 7 where it is compared to the tabulation of Gaur and Wunderlich.[41] The latter is based largely on extrapolation of experimental data on semicrystalline specimens to 100% crystallinity. Our calculated results are shown for both the heat capacity calculated from a one-dimensional dispersion curve on an isolated chain and that from the crystal three-dimensional curves. The divergence of the single chain based curve below ~150–200 K where the effect of the low-frequency skeletal vibrations coupling with the lattice modes becomes important is apparent. Above this temperature these vibrations have become classical. Above 300 K the calculated values begin to fall below the experiment values. This is no doubt due to the effects of anharmonicity in the lattice vibrations which are not addressed in the harmonic analysis underlying the calculations.

Table XII
Calculated Thermodynamic Functions of Hexagonal POM[a]

T	$-(G_T^0 - G_0^0)/T$	$(H_T^0 - H_0^0)/T$	S_T^0	C_P^0	C_V^0
2.00	0.139	0.042	0.181	0.062	0.041
4.00	0.175	0.066	0.241	0.128	0.085
6.00	0.209	0.106	0.314	0.250	0.187
8.00	0.246	0.164	0.411	0.443	0.359
10.00	0.292	0.247	0.538	0.721	0.615
12.00	0.346	0.356	0.701	1.090	0.964
14.00	0.410	0.492	0.902	1.544	1.396
16.00	0.487	0.656	1.142	2.068	1.899
18.00	0.574	0.844	1.419	2.645	2.456
20.00	0.674	1.055	1.729	3.258	3.047
22.0	0.785	1.284	2.069	3.888	3.657
24.00	0.907	1.527	2.435	4.523	4.271
26.00	1.040	1.782	2.822	5.152	4.878
28.00	1.181	2.045	3.226	5.766	5.471
30.00	1.331	2.313	3.644	6.361	6.045
32.00	1.490	2.584	4.073	6.933	6.596
34.00	1.654	2.856	4.510	7.481	7.123
36.00	1.825	3.128	4.953	8.004	7.624
38.00	2.001	3.397	5.399	8.502	8.102
40.00	2.183	3.665	5.847	8.976	8.555
50.00	3.139	4.941	8.080	11.033	10.507
60.00	4.144	6.099	10.243	12.682	12.050
70.00	5.164	7.141	12.306	14.068	13.331
80.00	6.181	8.084	14.264	15.273	14.431
90.00	7.183	8.944	16.127	16.369	15.421
100.00	8.167	9.739	17.906	17.399	16.346
110.00	9.130	10.481	19.611	18.393	17.235
120.00	10.073	11.181	21.254	19.365	18.101
130.00	10.994	11.848	22.841	20.320	18.950
140.00	11.896	12.487	24.382	21.265	19.790
150.00	12.778	13.104	25.881	22.204	20.624
160.00	13.643	13.702	27.344	23.130	21.445
170.00	14.491	14.284	28.774	24.059	22.269
180.00	15.324	14.853	30.175	24.989	23.093
190.00	16.142	15.412	31.552	25.924	23.922
200.00	16.946	15.960	32.906	26.855	24.749
210.00	17.738	16.503	34.240	27.792	25.580
220.00	18.518	17.037	35.553	28.736	26.419
230.00	19.287	17.566	36.854	29.689	27.266
240.00	20.047	18.091	38.135	30.650	28.121
250.00	20.795	18.613	39.405	31.619	28.985
260.00	21.536	19.132	40.666	32.596	29.857
270.00	22.268	19.649	41.917	33.582	30.738
280.00	22.993	20.164	43.154	34.575	31.625
290.00	23.707	20.678	44.389	35.573	32.518
300.00	24.418	21.192	45.611	36.576	33.416
310.00	25.121	21.704	46.825	37.583	34.317
320.00	25.818	22.216	48.033	38.590	35.219
330.00	26.510	22.727	49.236	39.596	36.120
340.00	27.196	23.238	50.436	40.603	37.021
350.00	27.877	23.749	51.626	41.613	37.926
360.00	28.553	24.260	52.809	42.622	38.830
370.00	29.225	24.769	53.993	43.621	39.723
380.00	29.892	25.278	55.170	44.613	40.610
390.00	30.555	25.788	56.338	45.598	41.489
400.00	31.215	26.297	57.506	46.575	42.362

[a] Units are J/mol of (CH_2O)–/K.

The calculated thermodynamic functions for POM are listed in Tables XII and XIII and displayed in Figure 8. As indicated in the introduction, there is some uncertainty in the experimentally derived values for crystalline hexagonal POM. This is not connected with the experimental values per se but rather with the extrapolation to 100% crystallinity. The values derived by Illers[9] are ~20% lower than the tabulation by Gaur and Wunderlich[6] at 300 K and about 8% lower at 175 K. A deviation plot of our calcu-

Table XIII
Calculated Thermodynamic Functions of Orthorhombic POM[a]

T	$-(G_T^0 - G_0^0)/T$	$(H_T^0 - H_0^0)/T$	S_T^0	C_P^0	C_V^0
2.00	0.023	0.024	0.048	0.049	0.007
4.00	0.048	0.049	0.097	0.103	0.019
6.00	0.073	0.078	0.151	0.170	0.045
8.00	0.100	0.112	0.211	0.257	0.090
10.00	0.129	0.152	0.281	0.377	0.168
12.00	0.161	0.203	0.365	0.545	0.294
14.00	0.198	0.268	0.465	0.774	0.481
16.00	0.238	0.349	0.587	1.065	0.730
18.00	0.285	0.447	0.732	1.421	1.044
20.00	0.338	0.565	0.903	1.837	1.418
22.00	0.398	0.702	1.100	2.302	1.841
24.00	0.466	0.856	1.321	2.803	2.300
26.00	0.541	1.026	1.566	3.330	2.786
28.00	0.624	1.210	1.833	3.871	3.285
30.00	0.713	1.405	2.119	4.418	3.790
32.00	0.810	1.611	2.421	4.964	4.294
34.00	0.915	1.824	2.739	5.503	4.791
36.00	1.025	2.043	3.068	6.030	5.277
38.00	1.142	2.267	3.408	6.545	5.749
40.00	1.264	2.493	3.757	7.044	6.207
50.00	1.943	3.635	5.578	9.295	8.248
60.00	2.704	4.740	7.444	11.181	9.925
70.00	3.514	5.780	9.293	12.808	11.343
80.00	4.350	6.750	11.099	14.254	12.580
90.00	5.197	7.658	12.855	15.584	13.700
100.00	6.049	8.514	14.564	16.838	14.745
110.00	6.899	9.326	16.226	18.046	15.743
120.00	7.744	10.103	17.847	19.219	16.708
130.00	8.582	10.849	19.430	20.365	17.645
140.00	9.413	11.568	20.981	21.496	18.565
150.00	10.235	12.268	22.502	22.611	19.471
160.00	11.049	12.950	23.998	23.707	20.358
170.00	11.854	13.614	25.468	24.802	21.243
180.00	12.650	14.267	26.915	25.888	22.119
190.00	13.439	14.908	28.342	26.980	23.003
200.00	14.220	15.538	29.756	28.066	23.879
210.00	14.993	16.163	31.151	29.152	24.756
220.00	15.758	16.776	32.534	30.243	25.638
230.00	16.517	17.385	33.906	31.337	26.523
240.00	17.272	17.989	35.258	32.438	27.414
250.00	18.017	18.590	36.604	33.543	28.310
260.00	18.757	19.187	37.945	34.658	29.216
270.00	19.494	19.780	39.273	35.777	30.125
280.00	20.225	20.371	40.592	36.901	31.039
290.00	20.948	20.962	41.912	38.027	31.956
300.00	21.671	21.549	43.218	39.155	32.875
310.00	22.387	22.133	44.522	40.286	33.797
320.00	23.097	22.720	45.818	41.417	34.719
330.00	23.806	23.304	47.109	42.546	35.639
340.00	24.511	23.886	48.401	43.673	36.556
350.00	25.212	24.467	49.678	44.803	37.477
360.00	25.907	25.047	50.957	45.929	38.394
370.00	26.603	25.627	52.226	47.046	39.301
380.00	27.294	26.206	53.501	48.153	40.199
390.00	27.980	26.783	54.762	49.252	41.089
400.00	28.667	27.359	56.021	50.345	51.972

[a] Units are J/mol of $-(CH_2O)-$/K.

lated values against the Gaur and Wunderlich[6] tabulation is shown in Figure 9. In the range 100–300 K our values lie within 4% of their tabulation and on average closer. Thus our results agree better with the Gaur and Wunderlich extrapolation than with that of Illers. However, the caveat must be entered that the thermal expansion used to correct our results to constant pressure is rather uncertain.

Electrooptical Results. As discussed in the preceeding paper, the mutual induction model used to calculate the electrostatic energy also permits a microscopic calculation of the high-frequency dielectric constant and refractive index. The results for PE have already been presented.[18]

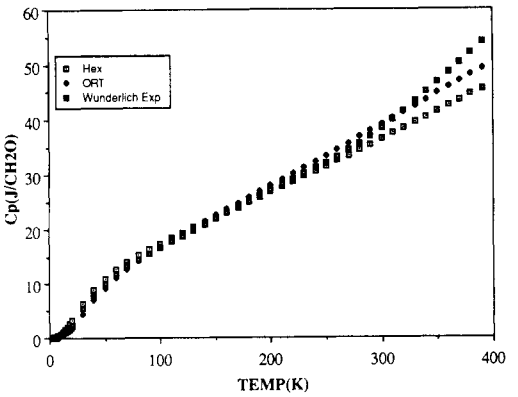

Figure 8. Heat capacity, C_p, versus temperature for poly(oxymethylene). Closed squares are taken from experimental data (hexagonal form) extrapolated to 100% crystallinity and tabulated by Gaur and Wunderlich.[6] The open squares are calculated from sampling 3D vibrational dispersion curves for hexagonal POM; diamonds are for orthorhombic POM.

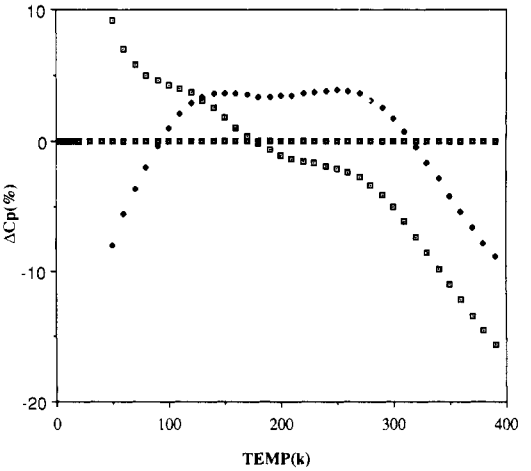

Figure 9. Deviation plot (in percent) of the calculated heat capacity of hexagonal and orthorhombic POM against the tabulation of Gaur and Wunderlich.[6]

For hexagonal POM we calculate $n_a = n_b = 1.42$ and $n_c = 1.69$ and for orthorhombic POM $n_a = 1.46$, $n_b = 1.44$, and $n_c = 1.67$.

Acknowledgment. We are indebted to the donors of the Petroleum Research Fund, administered by the American Chemical Society, and to the Polymers Program, Division of Materials Research of the National Science Foundation, for financial support of this work.

Registry No. PE, 9002-88-4; POM, 9002-81-7.

References and Notes

(1) Tadakoro, H.; Yasumoto, T.; Murahashi, S.; Nitta, I. *J. Polym. Sci.* **1960**, *44*, 266.
(2) Carazollo, G. A. *J. Polym. Sci., Part A* **1963**, *1*, 1573.
(3) Takahashi, Y.; Tadokoro, H. *J. Polym. Sci., Polym. Phys. Ed.* **1979**, *17*, 123.
(4) Carzollo, G.; Mammi, A. *J. Polym. Sci., Part A* **1963**, *1*, 965.
(5) Aich, R.; Haegele, P. C. *Prog. Colloid Polym. Sci.* **1985**, *71*, 86.
(6) Gaur, U.; Wunderlich, B. *J. Phys. Chem. Ref. Data* **1981**, *10*, 1001.
(7) Suzuki, H.; Grebowicz, J.; Wunderlich, B. *Makromol. Chem.* **1985**, *186*, 1109.
(8) Suzuki, H.; Wunderlich, B. *J. Polym. Sci., Polym. Phys. Ed.* **1985**, *23*, 1671.
(9) Illers, K. H. *Polym. Bull.* **1986**, *15*, 265.
(10) McCullough, R. L. In *Treatise on Materials Science and Technology*; Schultz, J. M. Ed.; Academic: New York, 1977; Vol. 10, part B.
(11) Halpin, J. C.; Kardos, J. L. *J. Appl. Phys.* **1972**, *43*, 2235.
(12) Boyd, R. H. *J. Polym. Sci., Polym. Phys. Ed.* **1983**, *21*, 493.
(13) Boyd, R. H.; Liau, W. B. *Macromolecules* **1986**, *19*, 2246.

(14) Schachtschneider, J. H.; Snyder, R. G. *Spectrochem. Acta* **1963**, *19*, 117.
(15) Snyder, R. G.; Schachtschneider, J. H. *Spectrochem. Acta* **1965**, *21*, 169.
(16) Snyder, R. G.; Zerbi, G. *Spectrochem. Acta* **1967**, *23A*, 391.
(17) Williams, D. E. *J. Chem. Phys.* **1966**, *45*, 3770; **1967**, *47*, 4680.
(18) Boyd, R. H.; Kesner, L. *Macromolecules* **1987**, *20*, 1802.
(19) Nelson, R. D., Jr.; Lide, D. R., Jr.; Maryott, A. A. *Natl. Stand. Ref. Data Ser. (U.S., Natl. Bur. Stand.)* **1967**, NSRDS-NBS 10.
(20) Astrup, E. E. *Acta Chem. Scand.* **1971**, *25*, 1494.
(21) Astrup, E. E. *Acta Chem. Scand.* **1973**, *27*, 3271.
(22) Sakakibara, M.; Yonemura, Y.; Matsuura, H.; Murata, H. *J. Mol. Struct.* **1980**, *66*, 333.
(23) Uchida, T.; Kurita, Y.; Kubo, M. *J. Polym. Sci.* **1956**, *19*, 365.
(24) Boyd, R. H. *J. Polym. Sci.* **1961**, *50*, 133.
(25) Flory, P. J. *Statistical Mechanics of Chain Molecules*; Wiley-Interscience: New York, 1969.
(26) Swan, P. R. *J. Polym. Sci.* **1962**, *56*, 403.
(27) Billmeyer, F. W. *J. Appl. Phys.* **1957**, *28*, 1114.
(28) Tasumi, M.; Krimm, S. *J. Chem. Phys.* **1967**, *46*, 755.
(29) Tadokoro, H. *Structure of Crystalline Polymers*; Wiley-Interscience: New York, 1979.
(30) Piseri, L.; Zerbi, G. *J. Chem. Phys.* **1968**, *48*, 3561.
(31) Wobser, G.; Blasenbrey, S. *Kolloid Z. Z. Polym.* **1970**, *241*, 985.
(32) Odajima, A.; Maeda, T. *J. Polym. Sci., Part C* **1966**, *15*, 55.
(33) Schaufele, R. F.; Shimanouchi, T. *J. Chem. Phys.* **1967**, *47*, 3605.
(34) Strobl, G. R.; Eckel, R. *J. Polym. Sci., Polym. Phys. Ed.* **1976**, *14*, 913.
(35) Snyder, R. G.; Krause, S. J.; Scherer, J. R. *J. Polym. Sci., Polym. Phys. Ed.* **1978**, *16*, 1593. Calculated from their frequency versus reciprocal lamellar thickness curve.
(36) Rabolt, J. F.; Fanconi, B. *J. Polym. Sci., Polym. Lett. Ed.* **1977**, *15*, 121.
(37) Kirkwood, J. G. *J. Chem. Phys.* **1939**, *7*, 506.
(38) Jungnitz, S.; Jakeways, R.; Ward, I. M. *Polymer* **1986**, *27*, 1651.
(39) Sham, T. P.; Newman, B. A.; Pae, K. D. *J. Mater. Sci.* **1977**, *12*, 771.
(40) Boyer, R. F. *Macromolecules* **1973**, *6*, 288.
(41) Gaur, U.; Wunderlich, B. *J. Phys. Chem. Ref. Data* **1981**, *10*, 119.

Dynamics of Semidilute Polymer Solutions: Hydrodynamic Screening

Y. Shiwa, Y. Oono,* and P. R. Baldwin

Department of Physics and Materials Research Laboratory, University of Illinois at Urbana—Champaign, Urbana, Illinois 61801. *Received June 11, 1987*

ABSTRACT: A study is made of the hydrodynamic screening effect on polymer solution dynamics in the semidilute regime. Starting from the time-dependent Ginzburg–Landau equations, the explicit crossover behavior of transport properties is calculated. Difficulties of existing theories are critically reviewed.

1. Introduction

A general theoretical framework for dynamics of nondilute polymer solutions (without entanglement) has been offered by Freed and Edwards.[1] The important aspect of the Freed–Edwards theory is that the presence of many polymer chains leads to a screening of the hydrodynamic interaction between the monomers of a polymer chain. However, almost no quantitative results have been produced with regard to the overall concentration dependence of the screening effect. This is especially true when the effect of the complicated interplay of the self-avoiding and hydrodynamic interactions is considered. Subsequently, Edwards and Muthukumar[2,3] devised a semiphenomenological framework to study good solutions. Later, Freed[4] proposed a supposedly more tractable version of the Edwards–Freed theory, but still almost no nontrivial quantitative results have been given. Furthermore, the above-mentioned models are not fully acceptable to statistical physicists, as the model describe the chains and the solvent at different levels of description; the chains at the kinetic level and the solvent at the hydrodynamic level.

We have proposed a new stochastic model,[5] which seems to offer a promising starting point for studying the crossover behavior of various dynamical quantities. Preliminary renormalization-group (RG) studies have been carried out on this model,[6] although these calculations cannot incorporate the hydrodynamic screening effect due to the approximations employed. In addition, the model yields the coupled integral equations for the effective polymer viscosity and monomer mobility;[5] however, the derivation is not a strict RG treatment. The formulas for viscosity and mobility happen to agree with those given by the Edwards–Freed theory. This, however, is not surprising because these formulas are sufficiently robust. The same coupled equations have been explored by Edwards, Muthukumar, and others.[1-3] However, their treatment has met considerable difficulties, perhaps because their treatment of equilibrium quantities in these equations is not reliable. For example, the approach used by Muthukumar and Edwards[2] does not give any natural overlapping parameter (see section 3) to be the most important parameter in the semidilute solution regime, so that their result is at variance with the general conclusions of the model they adopt and with experimental results.[7] This criticism is equally applicable to a theory of relaxation times,[3] which incorrectly identifies crucial parameters but fortuitously agrees with experiment. We fully analyze these coupled equations in this paper; the asymptotic results have already been published by one of the present authors.[5]

In section 2 we first describe our kinetic model equations and recapitulate the set of coupled equations. We present a derivation of those equations in the Appendix in the spirit of mode-coupling theory.[8] From these equations formulas for the solution viscosity and the hydrodynamic screening length are derived. In section 3 asymptotic results are derived. In section IV we proceed to solve the coupled equations explicitly. We obtain the crossover behavior (i.e., the overlap-parameter dependence) of the hydrodynamic screening length and the polymer viscosity with the aid of the known renormalization-group theoretical results[9] for semidilute solutions. The last section, 4, is a discussion and summary.

2. Model and General Results

In order to understand the nature of hydrodynamic screening effects, one needs a dynamical description of semidilute polymer solutions. We use a stochastic model[5]

0024-9297/88/2221-0208$01.50/0